Anti-influenza virus activity of benzo[d]thiazoles that target heat shock protein 90

Lamut, Andraž; Gjorgjieva, Marina; Naesens, Lieve; Liekens, Sandra; Lillsunde, Katja-Emilia ...

2020-05

Academic Press Inc.

http://hdl.handle.net/10138/341579

Lamut, A, Gjorgjieva, M, Naesens, L, Liekens, S, Lillsunde, K-E, Tammela, P, Kikelj, D & Tomaši, T 2020, 'Anti-influenza virus activity of benzo[d]thiazoles that target heat shock protein 90', Bioorganic Chemistry, vol. 98, 103733. https://doi.org/10.1016/j.bioorg.2020.103733

Anti-influenza virus activity of benzo[*d*]thiazoles that target heat shock protein 90

Andraž Lamut,[a] Marina Gjorgjieva,[a] Lieve Naesens,[b] Sandra Liekens,[b] Katja-Emilia Lillsunde,[c] Päivi Tammela,[c] Danijel Kikelj,[a] Tihomir Tomašič*,[a]

[a]University of Ljubljana, Faculty of Pharmacy, Aškerčeva 7, 1000 Ljubljana, Slovenia

[b]Rega Institute, KU Leuven, Herestraat 49, 3000 Leuven, Belgium

[c]Drug Research Programme, Division of Pharmaceutical Biosciences, Faculty of Pharmacy, University of Helsinki, P.O. Box 56, Viikinkaari 5EFI-00014, Finland

***Corresponding author: Tihomir Tomašič**

Faculty of Pharmacy

University of Ljubljana

Aškerčeva 7

SI-1000 Ljubljana, Slovenia

Tel: +386-1-4769556

E-mail: tihomir.tomasic@ffa.uni-lj.si

Abstract

Seasonal or pandemic influenza virus infections are a worldwide health problem requiring antiviral therapy. Since virus resistance to the established neuraminidase inhibitors and novel polymerase inhibitors is growing, new drug targets are needed. Heat shock protein 90 (Hsp90) is associated with several aspects of the influenza virus life cycle, and is considered a relevant host cell target. We report here on a series of benzo[*d*]thiazole and 4,5,6,7-tetrahydrobenzo[*d*]thiazole derivatives with robust and selective activities against influenza A (H1N1, H3N2) and influenza B viruses. Two compounds, **1** and **4**, have low micromolar EC_{50} values and show high binding affinities for Hsp90, which suggests that inhibition of Hsp90 is the mechanism underlying their antiviral effects. These compounds represent suitable scaffolds for designing novel Hsp90 inhibitors with favourable activities against influenza virus.

Keywords: antiviral agent; benzo[*d*]thiazole; Hsp90; influenza virus

1. Introduction

The World Health Organisation considers influenza pandemics as a major threat to global human health [1]. The severity of these pandemics varies greatly, from up to 400,000 fatalities in 2009 [2] to an estimated >50 million deaths in 1918 [3]. Besides, seasonal influenza infections cause each year 3 to 5 million severe cases [4] and 290,000-650,000 fatalities [5], the most vulnerable groups being the elderly, infants and people with chronic diseases. Influenza symptoms vary from mild upper respiratory tract disease to potentially lethal pneumonia, which can be caused by the virus itself or through secondary bacterial infection [6]. Since the widely used annual influenza vaccination [7] has limited effectiveness (<60%), antiviral medications are crucial to save the lives of high-risk populations.

The M2 ion channel blockers amantadine and rimantadine are no longer useful for the treatment of influenza due to global drug resistance [8]. The neuraminidase inhibitors oseltamivir and zanamivir are recommended for the treatment of severe influenza [9], as well as for pandemic preparedness [10]; however, also these drugs are prone to resistance [11]. Current drug development focuses heavily on the influenza virus polymerase, for which three inhibitors are now approved in a few countries or in advanced clinical evaluation: favipiravir, baloxavir and pimodivir [12, 13]. Mutant viruses showing resistance to baloxavir or pimodivir are frequently detected in the clinic [14, 15], implicating that the need remains for additional drugs with a high resistance barrier and another target, such as a host factor with a crucial role in virus replication.

Heat shock protein 90 (Hsp90) is a highly conserved and essential molecular chaperone [16] that has roles in cellular stress responses, intracellular protein transport, protein folding and degradation, and signal transduction. Although Hsp90 has been mainly explored as an anticancer target [17], it appears also relevant for antiviral drug development [18]. Most, if not all, viruses

require Hsp90 to form viral protein complexes during their replication [19]. Due to their high mutation rate, RNA viruses require the host chaperones to compensate for structural changes in viral protein assemblies and to ensure the activity of mutated proteins [19-21]. Hsp90 is present in four different isoforms in eukaryotic cells. The majority of viruses utilize two major cytoplasmic isoforms, namely Hsp90α and Hsp90β, for their proper replication and virulence [18, 22, 23]. Although both isoforms are important in viral life cycle, Hsp90β was shown to be more important in specific viruses [24-29]. In the case of influenza viruses an increased expression of Hsp90β was detected in infected cells upon infection with influenza A virus (IAV) [28] and Hsp90β was found to interact with mutated influenza B virus non-structural protein 1 (NS1) to promote formation of complex with viral polymerase basic protein 2 (PB2), which supports the formation of viral polymerase complex and leads to increased viral gene expression and enhancement of viral replication [29]. The potential advantages of targeting Hsp90 for antiviral therapy include [18, 30]: (i) lower risk of selection of drug-resistant viruses; (ii) potential for broad-spectrum antivirals; (iii) low toxicity in virus-infected animal models [31, 32]; (iv) favourable tissue distribution; and (v) reasonable tolerability for acute infections like influenza, as short-term administration would minimise possible adverse effects [19]. On the other hand, targeting the chaperoning function of a key host protein, such as Hsp90, could have some potential drawbacks. These include toxicity issues associated with the induction of heat shock response, which is one of the main reasons why Hsp90 inhibitors that have undergone clinical trials have not yet been approved for therapeutic use [30, 33, 34].

The activity of Hsp90 inhibitors for reduction of influenza A virus (IAV) replication in cell culture may occur at different stages in the viral replication cycle (Figure 1). First, Hsp90 can stimulate viral polymerase activity through interactions with the polymerase subunits and promotion of their assembly and nuclear import [35, 36]. Hsp90 inhibitors have been found to

reduce polymerase subunits half-life and inhibit their nuclear transport [37]. Secondly, Hsp90 promotes IAV-mediated apoptosis by activation of the caspase cascade, which is essential for virus replication, pathogenesis and virulence [38-41]. Thirdly, as Hsp90 was shown to prevent IAV neuraminidase degradation and to enhance its stability, Hsp90 inhibition decreases the levels of neuraminidase in infected cells [42, 43].

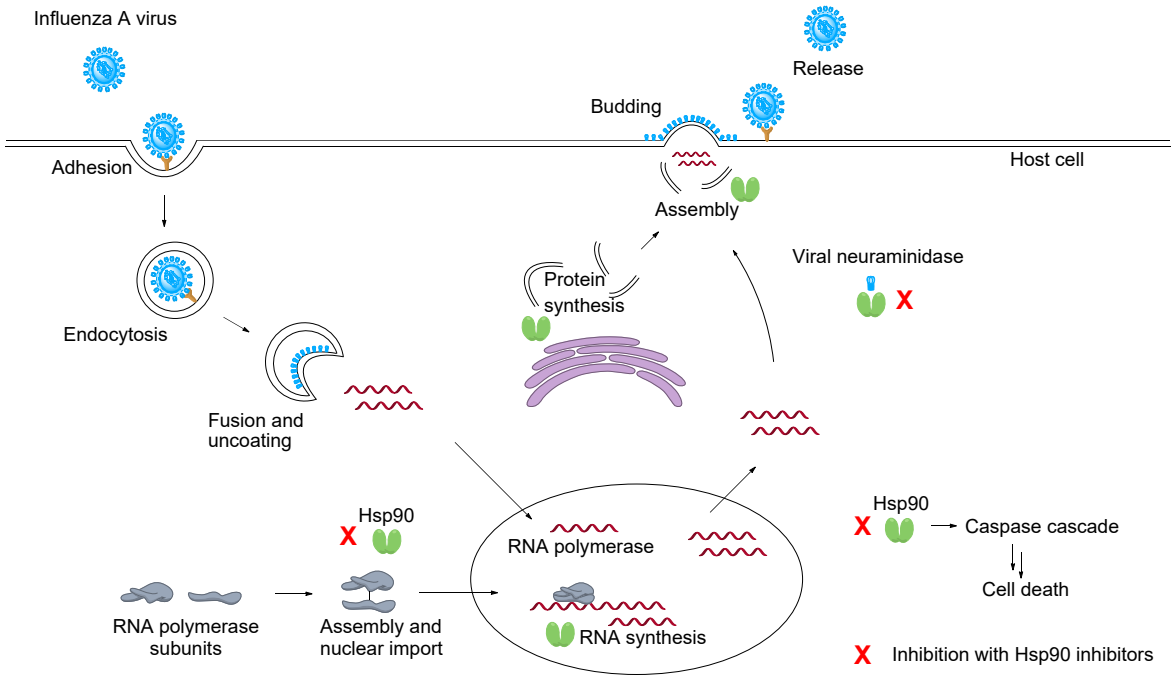

Figure 1. Hsp90 inhibitors can interfere with several aspects of the life cycle of the influenza A virus. Hsp90 enhances viral RNA synthesis by promoting assembly and nuclear import of the viral polymerase subunits. In addition, Hsp90 activates the caspase cascade, which leads to apoptosis, and it stabilises the IAV neuraminidase protein. Also, Hsp90 can participate in viral protein synthesis and assembly of viral particles [18, 39, 44].

After the discovery of the Hsp90 inhibitor geldanamycin, many other such inhibitors have been described, some of which have undergone phase III anticancer testing (Figure 2) [45-47]. This includes: structural analogues of geldanamycin, such as alvespimycin (17-DMAG), tanespimycin (17-AAG) and retaspimycin (IPI-504); the macrolide compounds radicicol and ganetespib

(STA9090); purine-based inhibitors such as Debio 0932; and the antibiotics novobiocin and coumermycin A1. Some of these Hsp90 inhibitors have been reported to show antiviral activity in cell culture. For example, geldanamycin and 17-AAG appear to inhibit replication of IAV and rhinoviruses, polioviruses and coxsackieviruses [44], while 17-DMAG inhibits Epstein-Barr virus and respiratory syncytial virus [18, 48]. Also, geldanamycin has been shown to reduce virus titres in Chikungunya-virus-infected mice [49].

In this report, we demonstrate the anti-influenza virus activity of compounds bearing a benzo[*d*]thiazole and 4,5,6,7-tetrahydrobenzo[*d*]thiazole scaffold, and we provide evidence that binding to Hsp90 is the likely mechanism that underlies these antiviral effects.

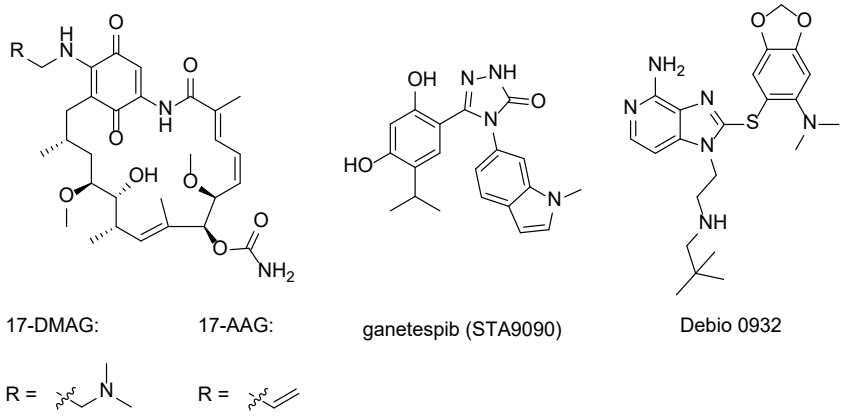

Figure 2. Representative Hsp90 inhibitors evaluated in clinical trials as anticancer agents.

2. Study design

We have previously reported that 4,5,6,7-tetrahydrobenzo[*d*]thiazoles that were originally designed as DNA gyrase B inhibitors can suppress hepatitis C virus replication, which appears to involve their binding to Hsp90 [50, 51]. Two other well-known DNA gyrase B inhibitors, novobiocin and coumermycin A1, also show inhibitory activities against Hsp90 and virus

replication [52-54]. Based on this, we evaluated here our 4,5,6,7-tetrahydrobenzo[*d*]thiazoles as well as a series of benzo[*d*]thiazole-based DNA gyrase B inhibitors [55] in terms of their inhibitory activities against the influenza A and B viruses. Moreover, binding of compounds displaying antiviral activity to the full-length Hsp90β was investigated by microscale thermophoresis.

The compound series here had either a dibromopyrrole or a dichloropyrrole moiety attached to position 6 of the central benzo[*d*]thiazole-2,6-diamine scaffold (Figure 3, type **I**). Considering position 2 of the benzo[*d*]thiazole core, oxalyl, malonyl and succinyl substituents were investigated, in the form of free carboxylic acids or their respective esters (ethyl or methyl). In addition, so-called 'reversed compounds' with the pyrrole moiety attached to position 2 of the benzo[*d*]thiazole scaffold were examined (Figure 3, type **II**). To investigate the importance of the benzene moiety, we also tested representative (*S*)-4,5,6,7-tetrahydrobenzo[*d*]thiazole-2,6-amine analogues (Figure 3, types **III**, **IV**). Moreover, we switched the amino group from position 6 to position 5 (Figure 3, type **V**), to determine the effects of this structural modification on the antiviral activity.

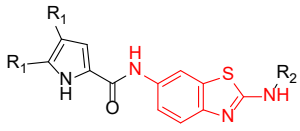

type **I**

13, R_1=Br, R_2=COCOOEt
14, R_1=Br, R_2=COCOOH
15, R_1=Br, R_2=$COCH_2COOMe$
16, R_1=Br, R_2=$COCH_2CH_2COOMe$
17, R_1=Br, R_2=$COCH_2CH_2COOH$
18, R_1=Cl, R_2=COCOOEt
19, R_1=Cl, R_2=$COCH_2COOMe$

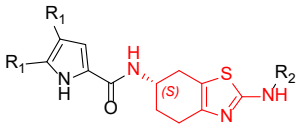

type **III**

21, R_1=Cl, R_2=COCOOEt
22, R_1=Cl, R_2=COCOOH
23, R_1=Cl, R_2=$COCH_2COOMe$
24, R_1=Cl, R_2=$COCH_2COOH$
25, R_1=Cl, R_2=$COCH_2CH_2COOMe$
26, R_1=Cl, R_2=$COCH_2CH_2COOH$
27, R_1=Br, R_2=$COCH_2COOMe$
28, R_1=Br, R_2=COCOOEt

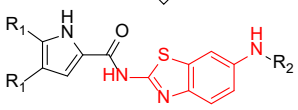

type **II**

1, R_1=Cl, R_2=H
2, R_1=Br, R_2=H
3, R_1=Cl, R_2=COCOOEt
4, R_1=Cl, R_2=COCOOH
5, R_1=Cl, R_2=$COCH_2COOMe$
6, R_1=Cl, R_2=$COCH_2COOH$
7, R_1=Cl, R_2=$COCH_2CH_2COOMe$
8, R_1=Cl, R_2=$COCH_2CH_2COOH$
9, R_1=Br, R_2=COCOOEt
10, R_1=Br, R_2=COCOOH
11, R_1=Br, R_2=$COCH_2COOMe$
12, R_1=Br, R_2=$COCH_2COOH$

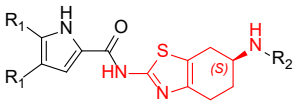

type **IV**

20, R_1=Br, R_2=COCOOEt
32, R_1=Br, R_2=H
33, R_1=Br, R_2=COCOOEt
34, R_1=Br, R_2=COCOOH

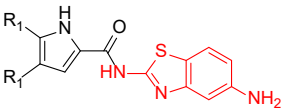

type **V**

36, R_1=Br
37, R_1=Cl

Figure 3. General structures of compounds evaluated for anti-influenza virus activity.

3. Chemistry

Synthesis of the benzo[*d*]thiazoles **1**-**19** and 4,5,6,7-tetrahydrobenzo[*d*]thiazoles **20**-**28** has been described previously [55-57]. Reversed 4,5,6,7-tetrahydrobenzo[*d*]thiazole analogues were prepared according to Scheme 1. (*S*)-4,5,6,7-tetrahydrobenzo[*d*]thiazole-2,6-diamine (**29**) was protected at the 6-amino group with the *tert*-butyloxycarbonyl (Boc) group to obtain **30**, which was coupled in the next step with 2,2,2-trichloro-1-(4,5-dichloro-1*H*-pyrrol-2-yl)ethan-1-one in the presence of Na_2CO_3 as a base at elevated temperature. The subsequent removal of Boc protection from **31** with 4 M HCl in 1,4-dioxane yielded compound **32**, which was then acylated with ethyl oxalyl chloride in the presence of 1,8-diazabicyclo[5.4.0]undec-7-ene (DBU), to obtain **33**. Finally, compound **34** was prepared by hydrolysis of **33** with 2 M NaOH in ethanol. Benzo[*d*]thiazoles were prepared by acylation of amine **35** by the 2,2,2-trichloro-1-(4,5-dibromo-1*H*-pyrrol-2-yl)ethan-1-one or 2,2,2-trichloro-1-(4,5-dichloro-1*H*-pyrrol-2-yl)ethan-1-one, in the presence of base at elevated temperature (Scheme 2) to yield compounds **36** and **37**.

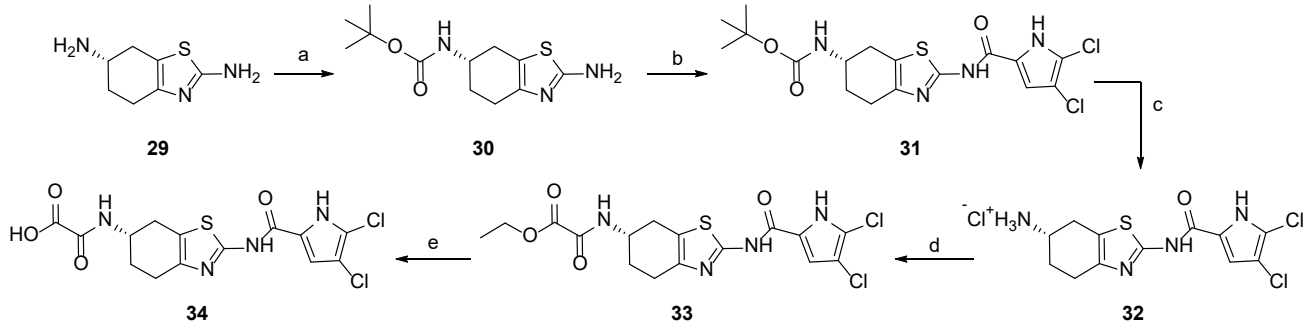

Scheme 1. Reagents and conditions: (*a*) BOC_2O in THF, 0 °C, 60 h, yield: 100 %; (*b*) 2,2,2-trichloro-1-(4,5-dichloro-

1*H*-pyrrol-2-yl)ethan-1-one, Na_2CO_3, DMF, 80 °C, 20 h, yield: 44 %; (*c*) 4 M HCl in 1,4-dioxane, 0 °C, 16 h, yield: 100 %; (*d*) ethyl oxalyl chloride, DBU, DMF, 0 °C, 3 h, yield: 35 %; (*e*) 2 M NaOH, EtOH, r.t., 3 h, yield: 64 %.

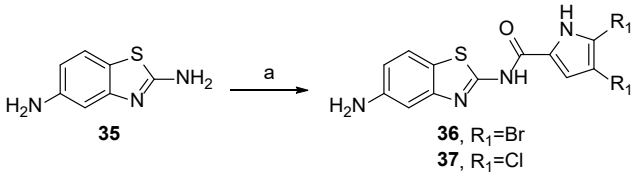

Scheme 2. Reagents and conditions: (*a*) for **36**: 2,2,2-trichloro-1-(4,5-dibromo-1*H*-pyrrol-2-yl)ethan-1-one; for **37**: 2,2,2-trichloro-1-(4,5-dichloro-1*H*-pyrrol-2-yl)ethan-1-one, Na_2CO_3, DMF, 80 °C, 20 h, yields: 38 % for **36** and 25 % for **37**.

4. Results and Discussion

4.1. Anti-influenza virus activity

We tested 33 compounds (Tables 1, 2) for their inhibitory activities against influenza A and B virus replication in Madin-Darby canine kidney (MDCK) cells. Antiviral activity was determined by using a cytopathic effect (CPE) reduction assay based on microscopic scoring, combined with the formazan-based (3-(4,5-dimethylthiazol-2-yl)-5-(3-carboxymethoxyphenyl)-2-(4-sulfophenyl)-2*H*-tetrazolium) (MTS) cell viability assay. These two methods were also used to determine compound cytotoxicity. These data are given in Tables 1 and 2.

In total, nine of 21 benzo[*d*]thiazoles (Table 1) and two of 12 4,5,6,7-tetrahydrobenzo-[*d*]thiazoles (Table 2) showed inhibitory activities against influenza virus. Similar antiviral EC_{50} values were obtained whether protection against virus-induced CPE was monitored by microscopy or by cell viability assay, and the EC_{50} values were comparable for influenza A virus (A/H1N1 and A/H3N2) and influenza B virus. The most potent compounds showed EC_{50} values in the range of 2 to 10 μM, and no cytotoxicity at 100 μM. Their potency was similar to that of the reference

compound ribavirin. This molecule acts on the cellular target IMP dehydrogenase, resulting in reduction of the intracellular GTP levels and inhibition of influenza virus replication [58]. However, as illustrated in Figure 4, the benzo[*d*]thiazole compounds suppressed the virus at non-toxic concentrations, which was not seen for ribavirin. Full inhibition of CPE was seen with compound **4** at 50 µM and ribavirin at 20 µM (Figure 4: compare panels A and B to the virus control in panel C). For ribavirin, this was associated with a clear cytostatic effect (panel E) whereas compound **4** showed no cytotoxicity at active concentrations (compare panel D to the cell control in panel F). Interestingly, the known Hsp90 inhibitor 17-DMAG included for comparison proved to be devoid of antiviral activity yet highly cytotoxic (CC_{50} value by MTS assay: 0.03 µM).

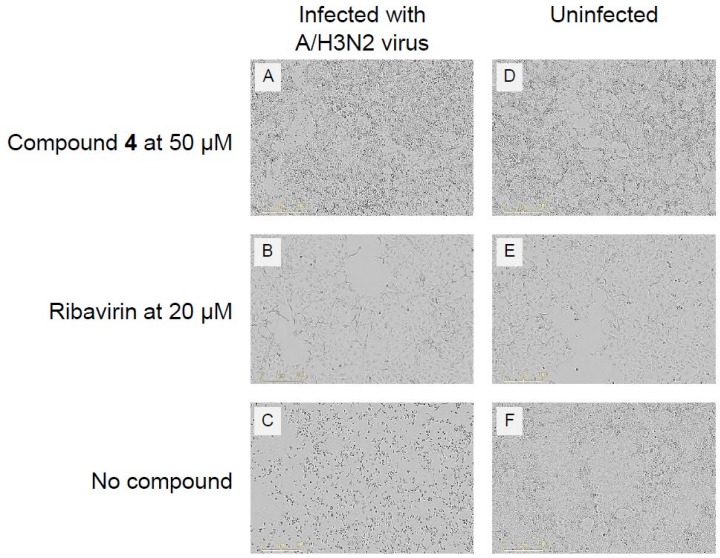

Figure 4. Compound **4** inhibits influenza virus-induced cytopathic effect at non-toxic concentrations.

Analysis of the structure-activity relationships for the benzo[*d*]thiazoles showed that all of these active compounds contained a pyrrole moiety attached to the 2-amino group of the central scaffold. In general, the dichloropyrrole derivatives had EC_{50} values that were a little lower than their corresponding dibromopyrrole-based counterparts, except for the malonyl acids **6** and **12**. Furthermore, the oxalyl esters **3** and **9** had comparable activities to their corresponding carboxylic

acids **4** and **10**, while they were a little more potent than their malonyl-substituted counterparts **6**, **7**, **11** and **12**. The succinyl-based analogues **7** and **8** were inactive. Moving the amino group from position 6, as in **1**, to position 5, as in **36** and **37**, abolished the antiviral activity.

Similar structure-activity relationships were seen for the 4,5,6,7-tetrahydrobenzo[*d*]thiazoles, as attachment of pyrrole to the 6-amino group resulted in inactive compounds, while compounds **33** and **34**, with dichloropyrrole attached to the 2-amino group, had moderate activities against the three influenza virus strains (Table 2, EC_{50} values, 16-100 μM). However, compounds **33** and **34** were less potent than their corresponding benzo[*d*]thiazole analogues **3** and **4**, which shows that the unsaturated benzo[*d*]thiazole ring is superior compared to the partially saturated 4,5,6,7-tetrahydrobenzo[*d*]thiazole moiety.

Table 1. Anti-influenza virus activities and Hsp90 binding affinities of the benzo[*d*]thiazole compounds.

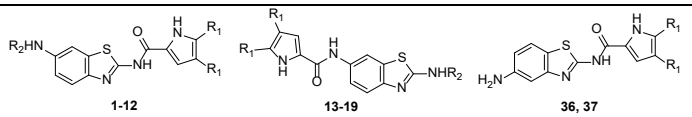

Compound	R_1	R_2	Anti-influenza virus assay in MDCK cells								Hsp90 binding (K_d; μM)
			Antiviral EC_{50} (μM)						Cytotoxicity (μM)		
			A/H1N1		A/H3N2		B				
			CPE	MTS	CPE	MTS	CPE	MTS	MCC	CC_{50}	
1	Cl	H	20	5.2	4	2.3	18	9.5	>100	>100	0.39 ±0.10
2	Br	H	NA	NA	NA	NA	NA	NA	>100	100	ND
3	Cl	COCOOEt	14	2.4	6.5	3.2	7.9	4.7	>100	>100	ND
4	Cl	COCOOH	11	3.9	8.4	2.6	22	17	>100	>100	0.26 ±0.04
5	Cl	$COCH_2COOMe$	50	31	9.5	7.8	45	43	>100	>100	6.4 ±1.6
6	Cl	$COCH_2COOH$	27	11	45	22	37	20	>100	>100	39 ±4.7
7	Cl	$COCH_2CH_2COOMe$	NA	NA	NA	NA	NA	NA	100	>100	ND
8	Cl	$COCH_2CH_2COOH$	NA	NA	NA	NA	NA	NA	100	>100	ND
9	Br	COCOOEt	15	3.5	9.5	6.6	16	9.4	>100	>100	ND
10	Br	COCOOH	34	10	22	3.8	40	19	>100	>100	16 ±1.5
11	Br	$COCH_2COOMe$	73	42	58	38	NA	45	>100	>100	17 ±2.8

12	Br	$COCH_2COOH$	15	13	31	32	27	9.6	>100	>100	51 ±7.4
13	Br	COCOOEt	NA	NA	NA	NA	NA	NA	100	54	ND
14	Br	COCOOH	NA	NA	NA	NA	NA	NA	20	18	ND
15	Br	$COCH_2COOMe$	NA	NA	NA	NA	NA	NA	20	15	ND
16	Br	$COCH_2CH_2COOMe$	NA	NA	NA	NA	NA	NA	4	10	ND
17	Br	$COCH_2CH_2COOH$	NA	NA	NA	NA	NA	NA	100	45	ND
18	Cl	COCOOEt	NA	NA	NA	NA	NA	NA	20	42	ND
19	Cl	$COCH_2COOMe$	NA	NA	NA	NA	NA	NA	100	>100	ND
36	Br	-	NA	NA	NA	NA	NA	NA	100	>100	ND
37	Cl	-	NA	NA	NA	NA	NA	NA	20	>100	ND
17-DMAG			NA	NA	NA	NA	NA	NA	>0.002	0.03	0.27 ± 0.02
Ribavirin	-	-	8.9	7.0	8.9	7.6	2.6	6.7	20	>100	
Zanamivir	-	-	0.8	0.4	0.5	1.5	0.4	0.8	>100	>100	
Amantadine	-	-	40	14	0.8	0.8	>200	>200	>200	>200	

CPE, cytopathic effect reduction assay (based on microscopic scoring); MTS, cell viability assays; MCC, minimum cytotoxic concentration; CC_{50}, 50% cytotoxic concentration; ND, not determined; NA, not active at subtoxic concentrations or the highest concentration tested, i.e. 100 μM for most compounds, 200 μM for amantadine and 10 μM for 17-DMAG.

Table 2. Anti-influenza virus activities and Hsp90 binding affinities of the 4,5,6,7-tetrahydrobenzo[*d*]thiazole compounds.

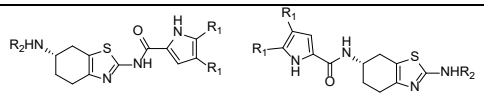

20, 32-34 **21-28**

Compound	**R_1**	**R_2**	**Anti-influenza virus assay in MDCK cells**								**Hsp90 binding (K_d; μM)**
			Antiviral EC_{50} (μM)						**Cytotoxicity (μM)**		
			A/H1N1		**A/H3N2**		**B**				
			CPE	**MTS**	**CPE**	**MTS**	**CPE**	**MTS**	**MCC**	**CC_{50}**	
20	Br	COCOOEt	NA	NA	NA	NA	NA	NA	>100	>100	ND
21	Cl	COCOOEt	NA	NA	NA	NA	NA	NA	100	51	ND
22	Cl	COCOOH	NA	NA	NA	NA	NA	NA	100	>100	ND
23	Cl	$COCH_2COOMe$	NA	NA	NA	NA	NA	NA	100	67	ND
24	Cl	$COCH_2COOH$	NA	NA	NA	NA	NA	NA	100	>100	ND
25	Cl	$COCH_2CH_2COOMe$	NA	NA	NA	NA	NA	NA	100	53	ND
26	Cl	$COCH_2CH_2COOH$	NA	NA	NA	NA	NA	NA	>100	>100	ND

27	Br	$COCH_2COOMe$	NA	NA	NA	NA	NA	NA	100	56	ND
28	Br	COCOOEt	NA	NA	NA	NA	NA	NA	>100	>100	ND
32	Cl	H	NA	NA	NA	NA	NA	NA	20	8.2	ND
33	Cl	COCOOEt	75	29	100	26	NA	59	>100	>100	16 ±2.4
34	Cl	COCOOH	46	17	42	16	79	54	>100	>100	31 ±6.6
17-DMAG			NA	NA	NA	NA	NA	NA	>0.002	0.03	0.27 ± 0.02
Ribavirin	-	-	8.9	7.0	8.9	7.6	2.6	6.7	20	>100	
Zanamivir	-	-	0.8	0.4	0.5	1.5	0.4	0.8	>100	>100	
Amantadine	-	-	40	14	0.8	0.8	NA	NA	>200	>200	

CPE, cytopathic effect reduction assays (based on microscopic scoring); MTS, cell viability assays; MCC, minimum cytotoxic concentration; CC_{50}, 50% cytotoxic concentration; ND, not determined; NA, not active at subtoxic concentrations or the highest concentration tested, i.e. 100 μM for most compounds, 200 μM for amantadine and 10 μM for 17-DMAG.

4.2. Binding of compounds to human Hsp90β

For the compounds that showed anti-influenza virus activities, their binding affinities to Hsp90β were determined using microscale thermophoresis: i.e., compounds **1**, **4-6**, **10-12**, **33**, **34**, (Tables 1, 2: right-hand column, for full data see Supporting Information, section 2). Due to aggregation issues, determination of affinity to Hsp90 was not possible for compounds **3** and **9**. Microscale thermophoresis is a biochemical method that monitors the movement of particles caused by a temperature gradient inside a thin glass capillary [59]. Among the tested compounds, **1** and **4** showed the highest binding affinities to Hsp90β, with K_d values of 0.39 μM and 0.26 μM, respectively. The other compounds had K_d values from 6.4 μM to 51 μM. The benzo[*d*]thiazole scaffold appeared to result in lower K_d values, as compound **4** (K_d = 0.26 μM) had a 120-fold higher Hsp90β binding affinity than its 4,5,6,7-tetrahydrobenzo[*d*]thiazole counterpart; i.e., compound **34** (K_d = 31 μM). Similarly, the dichloropyrrole moiety appeared to be favourable compared to the dibromopyrrole moiety, as **4** (K_d = 0.26 μM) was 60-fold more potent than **10** (K_d

= 16 μM). Whether compounds bind to the N-terminal ATP-binding site or C-terminal allosteric site of Hsp90β remains to be investigated.

5. Conclusions

Antiviral therapy for influenza virus infections has been dominated by neuraminidase inhibitors for many years but is currently expanding to include polymerase inhibitors. However, both drug classes are prone to selection of drug-resistant viruses, and so other therapeutic approaches are needed. We here focussed on Hsp90, a host cell factor with broad relevance for antiviral drug development. We identified several benzo[*d*]thiazole and a few 4,5,6,7-tetrahydrobenzo[*d*]thiazole compounds showing consistent activity against influenza A and B viruses, with some being equally potent yet more selective than ribavirin. The strong anti-influenza virus activity of compounds **1** and **4** was paralleled by superior binding affinities to Hsp90 suggesting that inhibition of Hsp90 is the likely mechanism behind the antiviral effect. Since inhibition of influenza virus was obtained in the absence of cytotoxicity, the benzo[*d*]thiazoles represent promising compounds for further optimisation and exploration of Hsp90 as a potential host cell target for influenza therapy.

6. Experimental

6.1. Materials and methods

The chemicals were obtained from Acros Organics (Geel, Belgium), Sigma-Aldrich (St. Louis, MO, USA), TCI Europe N.V. (Zwijndrecht, Belgium) and Apollo Scientific (Stockport, UK), and were used without further purification. Analytical TLC was performed on silica gel Merck 60 F_{254} plates (0.25 mm), with visualisation under UV light and with spray reagents. Column

chromatography was carried out on silica gel 60 (particle size, 240-400 mesh). HPLC analyses were performed on an Agilent Technologies 1100 instrument with a UV-Vis detector (G1365B), thermostat (G1316A), autosampler (G1313A) and C18 column (Zorbax Extend; 3.5 µm, 4.6 × 150 mm; Agilent). The following gradient elution methods were used: (*i*) with mobile phases A (0.1% trifluoroacetic acid in water) and B (methanol): 0-16 min, 40%-10% A; 16-21 min, 10% A; (*ii*) for compounds **36** and **37**, with mobile phases A and C (acetonitrile): 0-16 min, 95%-5% A; 16-21 min, 5% A. The flow rate was 1.0 mL/min, and the injection volume was 20 µL. All tested compounds were ≥95% pure by HPLC. Melting points were determined on a Reichert hot-stage microscope, and are uncorrected. ^{1}H and ^{13}C NMR spectra were recorded at 400 MHz and 100 MHz, respectively, on a spectrometer (AVANCE III 400; Bruker Corporation, Billerica, MA, USA) in dimethylsulphoxide (DMSO)-d_6 solutions, with TMS as the internal standard. Mass spectra were obtained using a compact mass spectrometer (expression series; Advion Inc., Ithaca, USA) and high resolution mass spectra were obtained using a mass spectrometer (Q-TOF Premier; Micromass, Waters, Manchester, UK; or Exactive Plus Orbitrap; Thermo Fischer Scientific Inc., Waltham, MA, USA). Optical rotations were measured on a polarimeter (241 MC; Perkin-Elmer). The reported values for specific rotation were the means of five successive measurements, using an integration time of 5 s. 2,2,2-Trichloro-1-(4,5-dichloro-1*H*-pyrrol-2-yl)ethan-1-one was synthesised and purified according to the previously reported procedure [60].

6.2. Synthetic procedures

tert-Butyl (S)-(2-amino-4,5,6,7-tetrahydrobenzo[d]thiazol-6-yl)carbamate (**30**) [61]. Starting compound (*S*)-4,5,6,7-tetrahydrobenzo[*d*]thiazole-2,6-diamine (**29**) (4.00 g; 23.6 mmol) was dissolved in tetrahydrofuran (THF) (30 mL) and cooled in an ice bath to 0 °C. Then di-*tert*-butyl dicarbonate (5.42 g, 24.8 mmol) dissolved in THF (15 mL) was added dropwise. The reaction

mixture was stirred for 60 h at room temperature. The solvent was removed under reduced pressure. Yield: 99.8% (6.35 g), pale brown amorphous solid. $[\alpha]_D^{25}$ −56.8 (c 0.42, MeOH). ^{1}H NMR (400 MHz, DMSO-d_6) δ 1.39 (s, 9H, 3 × CH_3), 1.52-1.68 (m, 1H, 5-CH_2), 1.80-1.90 (m, 1H, 5-CH_2), 2.30-2.48 (m, 3H, 4-CH_2, 7-CH_2), 2.69 (dd, $J_{7,7'}$ = 14.9 Hz, $J_{7,6}$ = 5.3 Hz, 1H, 7-CH_2), 3.57-3.70 (m, 1H, 6-CH), 6.65 (s, 2H, NH_2), 6.95 (d, J = 7.7 Hz, 1H, CONH) ppm. ^{13}C NMR (100 MHz, DMSO-d_6) δ 24.9, 28.2, 28.9, 46.8, 77.6, 112.4, 144.1, 154.9, 166.1 ppm. MS (ESI+): m/z = 292.4 ($[M + Na]^+$), 214.2 (100%).

tert-Butyl (S)-(2-(4,5-dichloro-1H-pyrrole-2-carboxamido)-4,5,6,7-tetrahydrobenzo[d]thiazol-6-yl)carbamate (**31**). Compound **30** (1.05 g, 3.91 mmol), 2,2,2-trichloro-1-(4,5-dichloro-1*H*-pyrrol-2-yl)ethan-1-one (1.10 g, 3.91 mmol) and sodium carbonate (0.414 g, 3.91 mmol) were dissolved in dry *N*,*N*-dimethylformamide (DMF) (15 mL). The reaction mixture was stirred for 20 h at 80 °C under argon. The solvent was removed under reduced pressure. The product precipitated after addition of a mixture of dichloromethane (50 mL) and saturated aqueous $NaHCO_3$ solution (30 mL). The precipitate was filtered and dried overnight at 60 °C. Yield: 44.1% (0.743 g), brown amorphous solid. $[\alpha]_D^{25}$ −48.9 (c 0.18, MeOH). ^{1}H NMR (400 MHz, DMSO-d_6) δ 1.40 (s, 9H, 3 × CH_3), 1.64-1.79 (m, 1H, 5-CH_2), 1.88-2.01 (m, 1H, 5-CH_2), 2.54-2.75 (m, 3H, 4-CH_2, 7-CH_2; signal partially overlaps with DMSO-d_5), 2.89 (dd, $J_{7,7'}$ = 15.7 Hz, $J_{7,6}$ = 4.4 Hz, 1H, 7-CH_2), 3.66-3.79 (m, 1H, 6-CH), 7.02 (d, J = 7.8 Hz, 1H, CONH), 7.16 (br s, 1H, pyrrole-H_3), 13.17 (br s, 1H, pyrrole-NH) ppm. ^{13}C NMR (100 MHz, DMSO-d_6) δ 24.5, 28.2, 28.5, 28.8, 46.5, 77.6, 107.6, 111.8, 116.6, 119.1, 124.2, 143.1, 155.0, 155.8, 157.6 ppm. MS (ESI+): m/z = 453.5 ($[M + Na]^+$, 100%).

(S)-2-(4,5-Dichloro-1H-pyrrole-2-carboxamido)-4,5,6,7-tetrahydrobenzo[d]thiazol-6-aminium chloride (**32**). Compound **31** (0.700 g, 1.62 mmol) was dissolved in 1,4-dioxane (5 mL) and cooled in an ice bath under an argon atmosphere. Then 4 M HCl solution in 1,4-dioxane (4.06 mL, 16.2

mmol) was added. The mixture was stirred overnight at room temperature. The solvent was removed under reduced pressure and dried. Yield: 100% (0.539 g), grey amorphous solid. $[\alpha]_D^{25}$ −14.6 (c 0.48, MeOH). ^{1}H NMR (400 MHz, DMSO-d_6) δ 1.87-2.01 (m, 1H, 5-CH_2), 2.12-2.22 (m, 1H, 5-CH_2), 2.69-2.85 (m, 3H, 4-CH_2, 7-CH_2), 3.11 (dd, $J_{7,7'}$ = 15.8 Hz, $J_{7,6}$ = 5.1 Hz, 1H, 7-CH_2), 7.38 (d, J = 2.8, 1H, pyrrole-H_3), 8.35 (d, J = 4.0, 3H, NH_3^+), 13.19 (d, J = 2.8, 1H, pyrrole-NH) ppm. ^{13}C NMR (100 MHz, DMSO-d_6) δ 23.5, 26.4, 26.6, 46.4, 108.9, 112.5, 117.6, 117.8, 122.6, 143.1, 156.3, 156.7 ppm. MS (ESI+): m/z = 331.4 ($[M + H]^+$), 170.2 (100%). HPLC: t_r = 10.58 min (96.7% at 254 nm).

Ethyl (S)-2-((2-(4,5-dichloro-1H-pyrrole-2-carboxamido)-4,5,6,7-tetrahydrobenzo[d]thiazol-6-yl)amino)-2-oxoacetate (**33**). Compound **32** (0.300 g, 0.813 mmol) was dissolved in DMF (10 mL) and 1,8-diazabicyclo[5.4.0]undec-7-ene (364 µL, 2.44 mmol) was added. The reaction mixture was cooled in an ice bath under an argon atmosphere. Then ethyl oxalyl chloride (118 µL, 1.06 mmol) was added dropwise. The dark brown solution was stirred at room temperature for 3 h. Then saturated aqueous $NaHCO_3$ solution (30 mL) and EtOAc (30 mL) were added. The white precipitate was filtered off. The organic phase was successively washed with saturated aqueous $NaHCO_3$ solution (2 × 30 mL), 10% citric acid (3 × 30 mL) and brine (30 mL), dried over sodium sulphate and filtered. The solvent was removed under reduced pressure and the crude product was purified by flash column chromatography using dichloromethane/ methanol (40:1) as eluent. Yield: 35.4% (0.124 g), pale brown amorphous solid. $[\alpha]_D^{25}$ −48.2 (c 0.15, MeOH). ^{1}H NMR (400 MHz, DMSO-d_6) δ 1.28 (t, J = 7.1 Hz, 3H, C$\underline{H_3}$CH_2), 1.84-2.01 (m, 2H, 5-CH_2), 2.64-2.79 (m, 3H, 4-CH_2, 7-CH_2), 2.93 (dd, $J_{7,7'}$ = 15.7 Hz, $J_{7,6}$ = 5.1 Hz, 1H, 7-CH_2), 4.04-4.15 (m, 1H, 6-CH), 4.25 (q, J = 7.1 Hz, 2H, $CH_3C\underline{H_2}$), 7.38 (s, 1H, pyrrole-H_3), 9.03 (d, J = 8.1 Hz, 1H, CONH), 12.26 (s, 1H, NHCO), 13.17 (s, 1H, pyrrole-NH) ppm. ^{13}C NMR (100 MHz, DMSO-d_6) δ 13.8, 24.4, 27.6,

28.0, 45.7, 62.0, 108.8, 112.3, 117.6, 156.9, 161.0 ppm. HRMS (ESI$^-$) *m/z* for $C_{16}H_{15}N_4O_4SCl_2$ ([M–H]$^-$): calcd 429.0191, found 429.0197. HPLC: t_r = 12.64 min (95.1% at 254 nm).

(S)-2-((2-(4,5-Dichloro-1H-pyrrole-2-carboxamido)-4,5,6,7-tetrahydrobenzo[d]thiazol-6-yl) amino-2-oxoacetic acid (**34**). Here, 2 M NaOH (0.348 mL, 0.696 mmol) was added to a solution of compound **33** (0.050 g, 0.116 mmol) in ethanol (3 mL). The reaction mixture was stirred at room temperature for 3 h and then the solvent was evaporated under reduced pressure. The crude product was dissolved in ethyl acetate (10 mL) and water (1 mL). The water phase was separated and acidified with 1 M HCl to pH 2. The pale brown precipitate was filtered off and dried under reduced pressure. Yield: 64.2% (0.030 g), pale grey amorphous solid. $[\alpha]_D^{25}$ −41.7 (c 0.241, MeOH). ^{1}H NMR (400 MHz, DMSO-d_6) δ 1.84-2.01 (m, 2H, 5-CH_2), 2.66-2.79 (m, 3H, 4-CH_2, 7-CH_2), 2.91 (dd, $J_{7,7'}$ = 15.6 Hz, $J_{7,6}$ = 5.3 Hz, 1H, 7-CH_2), 4.00-4.17 (m, 1H, 6-CH), 7.37 (d, J = 2.8 Hz, 1H, pyrrole-H_3), 8.96 (d, J = 8.2 Hz, 1H, CONH), 13.20 (d, J = 2.6 Hz, 1H, pyrrole-NH) ppm. ^{13}C NMR (100 MHz, DMSO-d_6) δ 24.5, 27.6, 28.0, 45.7, 108.8, 112.3, 117.5, 119.4, 122.8, 158.0, 162.2 ppm. HRMS (ESI$^-$) *m/z* for $C_{14}H_{11}N_4O_4SCl_2$ ([M–H]$^-$): calcd 400.9878, found 400.9872. HPLC: t_r = 11.44 min (98.8% at 254 nm).

General procedure A. A corresponding pyrrole (1 mmol) was dissolved in DMF (5 mL), and benzo[*d*]thiazole-2,5-diamine (**35**) (1 mmol) and Na_2CO_3 (1 mmol) were added. The mixture was stirred at 80 °C for 24 h. The reaction mixture was cooled and ethyl acetate (30 mL) was added. The organic phase was washed successively with 10% citric acid (2 × 20 mL), saturated aqueous $NaHCO_3$ solution (2 × 20 mL) and brine (20 mL). The organic phase was cooled in an ice bath and the precipitate formed was filtered off and dried at 60 °C.

N-(5-Aminobenzo[d]thiazol-2-yl)-4,5-dibromo-1H-pyrrole-2-carboxamide (**36**). Prepared from the benzo[*d*]thiazole-2,5-diamine (**35**) (100 mg, 0.61 mmol) and 2,2,2-trichloro-1-(4,5-dibromo-1*H*-pyrrol-2-yl)ethan-1-one (224 mg, 0.61 mmol) according to general procedure **A**. Yield 0.095 g

(38%); off white solid; m. p. 274–276 ºC; ^{1}H NMR (400 MHz, DMSO-d_6) δ 5.20 (br s, 2H, NH_2), 6.63 (dd, 1H, J_1 = 8.5 Hz, J_2 = 2.1 Hz, Ar-H), 6.91 (s, 1H, pyrrole-H), 7.44 (s, 1H, Ar-H), 7.55 (d, 1H, J = 8.5 Hz, Ar-H), 12.43 (br s, 1H, pyrrole-NH), 13.17 (br s, 1H, NHCO) ppm; ^{13}C NMR (100 MHz, DMSO-d_6) δ 98.3, 107.5, 112.1, 115.1, 120.8, 147.3 ppm; HRMS (ESI^-) *m/z* for $C_{12}H_7Br_2N_4OS$ ($[M-H]^-$): calcd 412.8707, found 412.8698; HPLC: t_r = 9.67 min (95.1% at 254 nm).

N-(5-Aminobenzo[d]thiazol-2-yl)-4,5-dichloro-1H-pyrrole-2-carboxamide (**37**). Prepared from the benzo[*d*]thiazole-2,5-diamine (**35**) (100 mg, 0.61 mmol) and 2,2,2-trichloro-1-(4,5-dichloro-1*H*-pyrrol-2-yl)ethan-1-one (170 mg, 0.61 mmol) according to general procedure **A**. Yield 0.050 g (25%); pale pink solid; m. p. 291–293 ºC; ^{1}H NMR (400 MHz, DMSO-d_6) δ 5.22 (br s, 2H, NH_2), 6.63 (dd, 1H, J_1 = 8.5 Hz, J_2 = 1.8 Hz, Ar-H), 6.92 (s, 1H, pyrrole-H), 7.46 (s, 1H, Ar-H), 7.55 (d, 1H, J = 8.3 Hz, Ar-H), 12.46 (s, 1H, pyrrole-NH), 13.24 (br s, 1H, NHCO) ppm; ^{13}C NMR (100 MHz, DMSO-d_6) δ 109.4, 113.1, 113.2, 118.4, 121.9, 148.4 ppm; HRMS (ESI^-) *m/z* for $C_{12}H_7Cl_2N_4OS$ ($[M-H]^-$): calcd 324.9718, found 324.9711; HPLC: t_r = 9.47 min (95.1% at 254 nm).

6.3. Microscale thermophoresis for binding to Hsp90β

The microscale thermophoresis assay has been previously reported [50, 51]. The well-known Hsp90 inhibitor 17-DMAG was included as the positive control. The compounds were dissolved in ethanol and diluted in microscale thermophoresis assay buffer (50 mM Tris-HCl, pH 7.4, 150 mM NaCl, 10 mM $MgCl_2$, 0.05% Tween-20, and 5% [v/v] ethanol) to concentrations of 0.003 μM to 100 μM (16 different concentrations) for each compound, and 0.0015 μM to 12.5 μM for 17-DMAG. Full-length human Hsp90β (GenBank Accession No. AY359878) with C-terminal His tag, MW = 83 kDa (Sigma- Aldrich Co., Saint Louis, MO, USA) was labelled using a Monolith NT™ Protein Labeling Kit RED-NHS (NanoTemper Technologies GmbH, Munich, Germany) according

to the manufacturer's labelling protocol. Labelled Hsp90β was carefully mixed with the compound dilutions to 35 nM final concentration of Hsp90β, and the mixtures were transferred into the capillaries (Monolith NT.115 premium-coated; NanoTemper Technologies GmbH). Measurements were carried out in a NanoTemper Monolith NT.115 instrument (NanoTemper Technologies GmbH). The measurements were performed at 20% LED and 20% MST power. The NT Analysis software (NanoTemper Technologies GmbH) was used for data analysis, which defined the dissociation constants (K_d; mean ±standard deviation), which were calculated on the basis of the thermophoresis and temperature jump data for three separate experiments.

For compounds **3**, **4** and **9**, the above procedure resulted in strong aggregation, and therefore the procedure was modified. These three compounds were prepared as 20 mM stocks in DMSO and retested in the microscale thermophoresis assay, at a final DMSO concentration of 0.25% in the assay buffer and the compound concentration range of 0.02 μM to 50 μM. This approach was successful for compound **4**, but not for **3** and **9**, for which the issue of aggregation was not solved.

6.4. Determination of antiviral activity against influenza viruses

The compounds were evaluated for inhibition of human influenza A/H1N1, A/H3N2 and B virus replication in MDCK cells, using a previously described CPE reduction assay [62, 63]. Semi-confluent MDCK cell cultures seeded in 96-well plates were infected with virus, and at the same time serial compound dilutions were added. To assess cytotoxicity, parallel plates were prepared receiving compounds but no virus. After three days incubation at 35 °C, virus-induced CPE and compound cytotoxicity were scored by microscopy. Next, the MTS cell viability reagent was added and 4 h later, absorbance at 490 nm was measured in a plate reader. Based on the CPE scores and MTS data in the virus-infected wells, the 50% effective concentration (EC_{50}) values were calculated assuming a semi-log dose response. Compound cytotoxicity was expressed as the

minimum cytotoxic concentration (MCC), i.e. the minimal concentration producing visible alterations in cell growth or morphology, such as rounding, cell lysis or shrinking. The MTS data from the uninfected plates were used to determine the 50% cytotoxic concentration (CC_{50}).

Associated content

Author information

Corresponding author: Tihomir Tomašič

*E-mail: Tihomir.tomasic@ffa.uni-lj.si; Tel: +386-1-4769556; Fax: +386-1-4258031.

Author contributions

The manuscript was written with contributions from all of the authors. All of the authors have read and approved to the final version of the manuscript.

Funding sources

This study was funded by the Slovenian Research Agency (Grant No. P1-0208, J1-1717, BI-US/18-19078) and Academy of Finland (Grant Nos. 277001, 304697, 312503).

Conflicts of interest

The authors declare that they have no conflicts of interest, including no financial, personal or other relationships with other people or organisations.

Acknowledgements

The authors wish to thank Dušan Žigon (Mass Spectrometry Centre, Jožef Stefan Institute, Ljubljana, Slovenia) for the mass spectra, Leentje Persoons and Nathalie Van Winkel for fine technical assistance, and Christopher Berrie for scientific editing of the manuscript.

References

[1] World Health Organization, Ten threats to global health in 2019. https://www.who.int/emergencies/ten-threats-to-global-health-in-2019, 2019 (accessed 10 October 2019).
[2] H.V. Fineberg, Pandemic preparedness and response-lessons from the H1N1 influenza of 2009. N. Engl. J. Med. 370 (2014) 1335-1342.
[3] J.K. Taubenberger, J.C. Kash, D.M. Morens, The 1918 influenza pandemic: 100 years of questions answered and unanswered. Sci. Transl. Med. 11 (2019) eaau5485.
[4] World Health Organization, Influenza (seasonal). https://www.who.int/news-room/fact-sheets/detail/influenza-(seasonal), 2018 (accessed 10 October 2019).
[5] A.D. Iuliano, K.M. Roguski, H.H. Chang, D.J. Muscatello, R. Palekar, S. Tempia, C. Cohen, J.M. Gran, D. Schanzer, B.J. Cowling, P. Wu, J. Kyncl, L.W. Ang, M. Park, M. Redlberger-Fritz, H. Yu, L. Espenhain, A. Krishnan, G. Emukule, L. van Asten, S. Pereira da Silva, S. Aungkulanon, U. Buchholz, M.A. Widdowson, J.S. Bresee, Estimates of global seasonal influenza-associated respiratory mortality: a modelling study, Lancet 391 (2018) 1285-1300.
[6] F. Krammer, G.J.D. Smith, R.A.M. Fouchier, M. Peiris, K. Kedzierska, P.C. Doherty, P. Palese, M.L. Shaw, J. Treanor, R.G. Webster, A. Garcia-Sastre, Influenza. Nat. Rev. Dis. Primers 4 (2018) 3.
[7] J.J. Treanor, Clinical practice. Influenza vaccination. N. Engl. J. Med. 375 (2016) 1261-1268.
[8] A. Moscona, Medical management of influenza infection. Annu. Rev. Med. 59 (2008) 397-413.
[9] J.S. Nguyen-Van-Tam, S. Venkatesan, S.G. Muthuri, P.R. Myles, Neuraminidase inhibitors: who, when, where? Clin. Microbiol. Infect. 21 (2015) 222-225.
[10] C.A. Russell, P.M. Kasson, R.O. Donis, S. Riley, J. Dunbar, A. Rambaut, J. Asher, S. Burke, C.T. Davis, R.J. Garten, S. Gnanakaran, S.I. Hay, S. Herfst, N.S. Lewis, J.O. Lloyd-Smith, C.A. Macken, S. Maurer-Stroh, E. Neuhaus, C.R. Parrish, K.M. Pepin, S.S. Shepard, D.L. Smith, D.L. Suarez, S.C. Trock, M.A. Widdowson, D.B. George, M. Lipsitch, J.D. Bloom, Improving pandemic influenza risk assessment. Elife 3 (2014) e03883.
[11] K. Thorlund, T. Awad, G. Boivin, L. Thabane, Systematic review of influenza resistance to the neuraminidase inhibitors. BMC Infect. Dis. 11 (2011) 134.
[12] A. Stevaert, L. Naesens, The influenza virus polymerase complex: an update on its structure, functions, and significance for antiviral drug design. Med. Res. Rev. 36 (2016) 1127-1173.
[13] L. Naesens, A. Stevaert, E. Vanderlinden, Antiviral therapies on the horizon for influenza. Curr. Opin. Pharmacol. 30 (2016) 106-115.
[14] F.G. Hayden, N. Sugaya, N. Hirotsu, N. Lee, M.D. de Jong, A.C. Hurt, T. Ishida, H. Sekino, K. Yamada, S. Portsmouth, K. Kawaguchi, T. Shishido, M. Arai, K. Tsuchiya, T. Uehara, A. Watanabe, G. Baloxavir Marboxil Investigators, Baloxavir marboxil for uncomplicated influenza in adults and adolescents. N. Engl. J. Med. 379 (2018) 913-923.

[15] R.W. Finberg, R. Lanno, D. Anderson, R. Fleischhackl, W. van Duijnhoven, R.S. Kauffman, T. Kosoglou, J. Vingerhoets, L. Leopold, Phase 2b study of pimodivir (JNJ-63623872) as monotherapy or in combination with oseltamivir for treatment of acute uncomplicated seasonal influenza A: TOPAZ Trial. J. Infect. Dis. 2019 (2018) 1026-1034.
[16] J. Li, J. Buchner, Structure, function and regulation of the Hsp90 machinery. Biomed. J. 36 (2013) 106-117.
[17] M.M. Biebl, J. Buchner, Structure, function, and regulation of the Hsp90 machinery. Cold Spring Harb. Perspect. Biol. 11 (2019) a034017.
[18] Y. Wang, F. Jin, R. Wang, F. Li, Y. Wu, K. Kitazato, Hsp90: a promising broad-spectrum antiviral drug target. Arch. Virol. 162 (2017) 3269-3282.
[19] R. Geller, S. Taguwa, J. Frydman, Broad action of Hsp90 as a host chaperone required for viral replication. Biochim. Biophys. Acta 1823 (2012) 698-706.
[20] S. Crowder, K. Kirkegaard, Trans-dominant inhibition of RNA viral replication can slow growth of drug-resistant viruses. Nat. Genet. 37 (2005) 701-709.
[21] A.M. Phillips, L.O. Gonzalez, E.E. Nekongo, A.I. Ponomarenko, S.M. McHugh, V.L. Butty, S.S. Levine, Y.S. Lin, L.A. Mirny, M.D. Shoulders, Host proteostasis modulates influenza evolution. Elife 6 (2017) e28652.
[22] A.S. Sreedhar, E. Kalmar, P. Csermely, Y.F. Shen, Hsp90 isoforms: functions, expression and clinical importance. FEBS Lett. 562 (2004) 11-15.
[23] Y. Wang, R. Wang, F. Li, Z. Zhang, Q. Wang, Z. Ren, F. Jin, K. Kitazato, Heat-shock protein 90alpha is involved in maintaining the stability of VP16 and VP16-mediated transactivation of alpha genes from herpes simplex virus-1. Mol. Med. 24 (2018) 65.
[24] C.Y. Hung, M.C. Tsai, Y.P. Wu, R.Y. Wang, Identification of heat-shock protein 90 beta in Japanese encephalitis virus-induced secretion proteins. J. Gen. Virol. 92 (2011) 2803-2809.
[25] R.Y. Wang, R.L. Kuo, W.C. Ma, H.I. Huang, J.S. Yu, S.M. Yen, C.R. Huang, S.R. Shih, Heat shock protein-90-beta facilitates enterovirus 71 viral particles assembly. Virology 443 (2013) 236-247.
[26] Y.L. Tsou, Y.W. Lin, H.W. Chang, H.Y. Lin, H.Y. Shao, S.L. Yu, C.C. Liu, E. Chitra, C. Sia, Y.H. Chow, Heat shock protein 90: role in enterovirus 71 entry and assembly and potential target for therapy. PLoS One 8 (2013) e77133.
[27] Y. Wang, Y. Li, T. Ding, Heat shock protein 90beta in the Vero cell membrane binds Japanese encephalitis virus. Int. J. Mol. Med. 40 (2017) 474-482.
[28] A. Wahl, F. Schafer, W. Bardet, W.H. Hildebrand, HLA class I molecules reflect an altered host proteome after influenza virus infection. Hum. Immunol. 71 (2010) 14-22.
[29] A. Sadewasser, S. Saenger, K. Paki, T. Schwecke, T. Wolff, Disruption of Src homology 3-binding motif within non-structural protein 1 of influenza B virus unexpectedly enhances viral replication in human cells. J. Gen. Virol. 97 (2016) 2856-2867.
[30] Y.L. Wang, F.J. Jin, F. Li, S.R. Qin, Y.F. Wang, Could targeting the heat shock protein 90 revolutionize antiviral therapy? Future Virol. 13 (2018) 119-127.
[31] R. Geller, M. Vignuzzi, R. Andino, J. Frydman, Evolutionary constraints on chaperone-mediated folding provide an antiviral approach refractory to development of drug resistance. Genes Dev. 21 (2007) 195-205.
[32] S. Nakagawa, T. Umehara, C. Matsuda, S. Kuge, M. Sudoh, M. Kohara, Hsp90 inhibitors suppress HCV replication in replicon cells and humanized liver mice. Biochem. Biophys. Res. Commun. 353 (2007) 882-888.

[33] J. McConnell, Y. Wang, S. McAlpine, Targeting the C-terminus of Hsp90 as a cancer therapy. In: McAlpine S., Edkins A. (eds) Heat shock protein inhibitors. Topics in Medicinal Chemistry, vol 19. Springer, Cham, 2015, 1-22.
[34] D. Bickel, H. Gohlke, C-terminal modulators of heat shock protein of 90kDa (Hsp90): State of development and modes of action. Bioorg. Med. Chem. 27 (2019) 115080.
[35] F. Momose, T. Naito, K. Yano, S. Sugimoto, Y. Morikawa, K. Nagata, Identification of Hsp90 as a stimulatory host factor involved in influenza virus RNA synthesis. J. Biol. Chem. 277 (2002) 45306-45314.
[36] T. Naito, F. Momose, A. Kawaguchi, K. Nagata, Involvement of Hsp90 in assembly and nuclear import of influenza virus RNA polymerase subunits. J. Virol. 81 (2007) 1339-1349.
[37] G. Chase, T. Deng, E. Fodor, B.W. Leung, D. Mayer, M. Schwemmle, G. Brownlee, Hsp90 inhibitors reduce influenza virus replication in cell culture. Virology 377 (2008) 431-439.
[38] C. Zhang, Y. Yang, X. Zhou, Z. Yang, X. Liu, Z. Cao, H. Song, Y. He, P. Huang, The NS1 protein of influenza A virus interacts with heat shock protein Hsp90 in human alveolar basal epithelial cells: implication for virus-induced apoptosis. Virol. J. 8 (2011) 181.
[39] M. Marques, B. Ramos, A.R. Soares, D. Ribeiro, Cellular proteostasis during influenza A virus infection-friend or foe? Cells 8 (2019) e228.
[40] S. Ludwig, S. Pleschka, O. Planz, T. Wolff, Ringing the alarm bells: signalling and apoptosis in influenza virus infected cells. Cell Microbiol. 8 (2006) 375-386.
[41] E.W. Brydon, S.J. Morris, C. Sweet, Role of apoptosis and cytokines in influenza virus morbidity, FEMS Microbiol. Rev. 29 (2005) 837-850.
[42] P. Gaur, P. Ranjan, S. Sharma, J.R. Patel, J.B. Bowzard, S.K. Rahman, R. Kumari, S. Gangappa, J.M. Katz, N.J. Cox, R.B. Lal, S. Sambhara, S.K. Lal, Influenza A virus neuraminidase protein enhances cell survival through interaction with carcinoembryonic antigen-related cell adhesion molecule 6 (CEACAM6) protein. J. Biol. Chem. 287 (2012) 15109-15117.
[43] P. Kumar, P. Gaur, R. Kumari, S.K. Lal, Influenza A virus neuraminidase protein interacts with Hsp90, to stabilize itself and enhance cell survival. J. Cell. Biochem. 120 (2019) 6449-6458.
[44] M.K. Howe, T.A.J. Haystead, New indications for HSP90 and HSP70 inhibitors as antiviral drugs. In: Asea A., Almasoud N., Krishnan S., Kaur P. (eds) Heat shock protein-based therapies. Heat Shock Proteins, vol 9. Springer, Cham, 2015, 175-196.
[45] K. Jhaveri, T. Taldone, S. Modi, G. Chiosis, Advances in the clinical development of heat shock protein 90 (Hsp90) inhibitors in cancers. Biochim. Biophys. Acta 1823 (2012) 742-755.
[46] D.M. Ramsey, R.R.A. Kitson, J.I. Levin, C.J. Moody, S.R. McAlpine, Recent advances in macrocyclic Hsp90 inhibitors, in: J. Levin (Ed.), Macrocycles in Drug Discovery, The Royal Society of Chemistry, Cambridge, 2015, pp. 37-77.
[47] R. Bhat, S.R. Tummalapalli, D.P. Rotella, Progress in the discovery and development of heat shock protein 90 (Hsp90) inhibitors. J. Med. Chem. 57 (2014) 8718-8728.
[48] X. Sun, J.A. Bristol, S. Iwahori, S.R. Hagemeier, Q. Meng, E.A. Barlow, J.D. Fingeroth, V.L. Tarakanova, R.F. Kalejta, S.C. Kenney, Hsp90 inhibitor 17-DMAG decreases expression of conserved herpesvirus protein kinases and reduces virus production in Epstein-Barr virus-infected cells. J. Virol. 87 (2013) 10126-10138.
[49] A.P. Rathore, T. Haystead, P.K. Das, A. Merits, M.L. Ng, S.G. Vasudevan, Chikungunya virus nsP3 & nsP4 interacts with HSP-90 to promote virus replication: HSP-90 inhibitors reduce CHIKV infection and inflammation in vivo, Antiviral Res. 103 (2014) 7-16.
[50] K.E. Lillsunde, T. Tomašič, D. Kikelj, P. Tammela, Marine alkaloid oroidin analogues with antiviral potential: A novel class of synthetic compounds targeting the cellular chaperone Hsp90. Chem. Biol. Drug. Des. 90 (2017) 1147-1154

[51] K.E. Lillsunde, T. Tomašič, P. Schult, V. Lohmann, D. Kikelj, P. Tammela, Inhibition of hepatitis C replication by targeting the molecular chaperone Hsp90: synthesis and biological evaluation of 4,5,6,7-tetrahydrobenzo[1,2-*d*]thiazole derivatives, ChemMedChem. 14 (2019) 334-342.
[52] L. Vozzolo, B. Loh, P.J. Gane, M. Tribak, L. Zhou, I. Anderson, E. Nyakatura, R.G. Jenner, D. Selwood, A. Fassati, Gyrase B inhibitor impairs HIV-1 replication by targeting Hsp90 and the capsid protein. J. Biol. Chem. 285 (2010) 39314-39328.
[53] J.A. Burlison, B.S. Blagg, Synthesis and evaluation of coumermycin A1 analogues that inhibit the Hsp90 protein folding machinery. Org. Lett. 8 (2006) 4855-4858.
[54] J.A. Burlison, L. Neckers, A.B. Smith, A. Maxwell, B.S. Blagg, Novobiocin: redesigning a DNA gyrase inhibitor for selective inhibition of Hsp90. J. Am. Chem. Soc. 128 (2006) 15529-15536.
[55] M. Gjorgjieva, T. Tomašič, M. Barančokova, S. Katsamakas, J. Ilaš, P. Tammela, L. Peterlin Mašič, D. Kikelj, Discovery of benzothiazole scaffold-based DNA gyrase B inhibitors, J. Med. Chem. 59 (2016) 8941-8954.
[56] T. Tomašič, S. Katsamakas, Ž. Hodnik, J. Ilaš, M. Brvar, T. Šolmajer, S. Montalvao, P. Tammela, M. Banjanac, G. Ergović, M. Anderluh, L. Peterlin Mašič, D. Kikelj, Discovery of 4,5,6,7-tetrahydrobenzo[1,2-*d*]thiazoles as novel DNA gyrase inhibitors targeting the ATP-binding site, J. Med. Chem. 58 (2015) 5501-5521.
[57] T. Tomašič, M. Mirt, M. Barančokova, J. Ilaš, N. Zidar, P. Tammela, D. Kikelj, Design, synthesis and biological evaluation of 4,5-dibromo-*N*-(thiazol-2-yl)-1*H*-pyrrole-2-carboxamide derivatives as novel DNA gyrase inhibitors, Bioorg. Med. Chem. 25 (2017) 338-349.
[58] E. Vanderlinden, B. Vrancken, J. Van Houdt, V.K. Rajwanshi, S. Gillemot, G. Andrei, P. Lemey, L. Naesens, Distinct effects of T-705 (favipiravir) and ribavirin on influenza virus replication and viral RNA synthesis, Antimicrob. Agents Chemother. 60 (2016) 6679-6691.
[59] M.G. Plach, K. Grasser, T. Schubert, Microscale thermophoresis as a tool to study protein-peptide interactions in the context of large eukaryotic protein complexes. Bio-Protocol. 7 (2017) e2632.
[60] S. Guiheneuf, L. Paquin, F. Carreaux, E. Durieu, L. Meijer, J.P. Bazureau, An efficient approach to dispacamide A and its derivatives, Org. Biomol. Chem. 10 (2012) 978-987.
[61] D.S. Prasanna, C.V. Kavitha, K. Vinaya, S.R. Ranganatha, S.C. Raghavan, K.S. Rangappa, Synthesis and identification of a new class of antileukemic agents containing 2-(arylcarboxamide)-(*S*)-6-amino-4,5,6,7-tetrahydrobenzo[*d*]thiazole. Eur. J. Med. Chem. 45 (2010) 5331-5336.
[62] L. Naesens, E. Vanderlinden, E. Roth, J. Jeko, G. Andrei, R. Snoeck, C. Pannecouque, E. Illyes, G. Batta, P. Herczegh, F. Sztaricskai, Anti-influenza virus activity and structure-activity relationship of aglycoristocetin derivatives with cyclobutenedione carrying hydrophobic chains. Antiviral. Res. 82 (2009) 89-94.
[63] P. Vrijens, S. Noppen, T. Boogaerts, E. Vanstreels, R. Ronca, P. Chiodelli, M. Laporte, E. Vanderlinden, S. Liekens, A. Stevaert, L. Naesens, Influenza virus entry via the GM3 ganglioside-mediated platelet-derived growth factor receptor beta signalling pathway. J. Gen. Virol. 100 (2019) 583-601.